

## Effect of Seismic Loading on Porewater Pressure in Clayey Soil under Disconnected Piles-Raft Foundation

Sajjad Riyadh Nafel<sup>1,\*</sup>, Mahdi Obaed Karkush<sup>2</sup>

Department of Civil Engineering, College of Engineering, University of Baghdad, Baghdad, Iraq.  
[sajjad.nafil2001m@coeng.uobaghdad.edu.iq](mailto:sajjad.nafil2001m@coeng.uobaghdad.edu.iq)<sup>1</sup>, [mahdi\\_karkush@coeng.uobaghdad.edu.iq](mailto:mahdi_karkush@coeng.uobaghdad.edu.iq)<sup>2</sup>

### ABSTRACT

The disconnected piled raft foundation (DCPRF) is one of the newly introduced foundations for specialization in geotechnical engineering, which significantly reduces the moment and stress on the pile head. In addition, this type of foundation is an ideal choice in areas with seismic activity due to the presence of cushion material between the raft and the piles. This work aims to present a numerical model in PLAXIS 3D software for connected piled raft and disconnected piled raft foundations under the influence of seismic loads and investigate the effect of pore water pressure on the disconnected foundation compared to the connected foundation. The study will depend on the earthquake that struck Iraq in November 2017 in the Halabja region. Strength was 7.3 on the Richter scale with PGA (0.1g). The results of changing pore water pressure showed the variation of pore water pressure. In the case of a DCPRF, the porewater pressure and excess porewater pressure in the soil are much greater than in the case of a CPRF. The increase in the porewater pressure is due to the weight of the building and the weight of the additional cushion layer on the soil. The mechanism for transferring the load in the case of a DCPRF is carried out by raft, then to the cushion, and then to the soil and piles. The load transferred to the soil in the case of DCPRF is more than that transferred to the soil in the CPRF system.

**Keywords:** Connected piled raft, Disconnected piled raft, Cushion, Seismic loading, Numerical analysis.

---

\*Corresponding author

Peer review under the responsibility of University of Baghdad.

<https://doi.org/10.31026/j.eng.2024.03.06>

This is an open access article under the CC BY 4 license (<http://creativecommons.org/licenses/by/4.0/>).

Article received: 22/11/2022

Article accepted: 04/12/2023

Article published: 01/03/2024



# تأثير الحمل الزلزالي على ضغط ماء المسام في التربة الطينية تحت اساس حصيري منفصل عن الركائز

سجاد رياض نافل<sup>\*</sup>، مهدي عبيد كركوش

قسم الهندسة المدنية، كلية الهندسة، جامعة بغداد، بغداد، العراق

## الخلاصة

يعد أساس الحصييره المدعم بالركائز المنفصلة (DCPRF) أحد الأسس التي تم إدخالها حديثاً التخصص في الهندسة الجيوتقنية مما يقلل بشكل كبير من العزوم والضغط على رأس الركائز. بالإضافة إلى ذلك، يعتبر هذا النوع من الأساس اختياراً مثالياً في المناطق ذات النشاط الزلزالي نظراً لوجود طبقة الوسادة بين الحصييره والركائز. الهدف من هذا البحث هو تقديم نموذج رقمي في برنامج PLAXIS 3D لأساس الحصييره المتصلة بالركائز وأساس الحصييره المنفصلة عن الركائز تحت تأثير الأحمال الزلزالية والتحقيق في تأثير ضغط المياه المسامية على الأساس المنفصل مقارنة بالأساس المتصل. ستعتمد الدراسة على الزلزال الذي ضرب العراق في تشرين الثاني 2017 في منطقة حلبجة. كانت القوة 7.3 على مقياس ريختر مع اعظم قيمه للتعجيل (0.1 جم). أظهرت النتائج تغيير ضغط ماء المسام مع اختلاف نوع الاساس. حيث لوحظ في حالة DCPRF أن ضغط ماء المسام وضغط ماء المسام الزائد في التربة أكبر بكثير من حالة CPRF. تعود الزيادة في ضغط ماء المسام إلى وزن المبنى ووزن طبقة الوسادة الإضافية على التربة. حيث تكون آلية نقل الحمل في حالة DCPRF بواسطة الأساس الحصييري ثم إلى طبقه الوسادة، ثم إلى التربة والركائز. أن الأحمال المنقولة إلى التربة في حالة DCPRF أكبر من تلك المنقولة إلى التربة في نظام CPRF.

**الكلمات المفتاحية:** أساس حصيري مع ركائز متصلة، أساس حصيري مع ركائز منفصلة، الوسادة، تحميل زلزالي، تحليل عددي.

## 1. INTRODUCTION

When the raft's bearing capacity is sufficient to sustain the superstructure, but the raft's total and differential settlements exceed the allowable limit, a small number of piles can be used to control the settlements (Burland, 1977; Karkush and Ala, 2019; Karkush and Aljorany, 2020; Karkush et al., 2020). The pile heads are usually structurally connected to the raft to make a rigid connection. These piles should have sufficient bearing capacity and safety factors to avoid structural failure (AL-Mosawe et al., 2007; Al-Kinani et al., 2020; AL-Jeznawi et al., 2022). Because high axial stress can be developed in piles and lateral forces from wind and earthquakes can destroy connections, even though structural failure can be prevented by using high-strength materials with a high factor of safety, this technique may be uneconomical. A new solution for solving such concerns has recently been presented (Zhao, 1998). It involves isolating the raft from the pile with soil material that is strong enough to sustain the stresses imposed on it while also preventing or reducing loads of seismic waves or shear forces on the pile's head. This void may be filled with a suitable substance, which can be selected depending on the circumstances (Wong et al., 2000). Since the piles are not structurally attached to the raft, a smaller factor of safety may be utilized to protect the pile materials and prevent structural damage (as low as 1.3) (Wong et al., 2000; Karkush et al., 2022). The result obtained from the previous works proved that the disconnected piled raft contains a cushion between the pile and the raft and carries more



loads than the connected piled raft foundation. At the same time, carrying the loads with the connected piled raft may be greater, and this method leads to more economical results than others. Also, disconnected piles can be used in buildings subjected to high horizontal loads such as earthquakes or winds, especially in buildings containing basements and with weak soil that needs strengthening, such as river sidewalks and ports **(Shafique et al., 2017)**.

This cushion is considered a layer that transfers the loads to the soil and the piles below the mat and contributes to a certain amount of bearing the loads and the way of distributing the loads on the piles **(Fioravante, 2011)**. This research was devoted to studying the effect of porewater pressure on the disconnected piled raft foundation under seismic loading and comparing the results with the connected piled raft foundation under the same loading **(Sharma, 2017)**.

This work aims to present a numerical model in PLAXIS 3D software for the connected and disconnected piled raft foundations under the influence of seismic loads. The effect of pore water pressure on the disconnected foundation compared to the connected foundation is investigated. The effect of a layer of sand placed between the piles and the raft in an unconnected piled raft system as a cushion layer is studied in terms of its thickness and the reinforcement with geogrid.

## 2. NUMERICAL MODELLING

In various geotechnical applications, numerical modelling is commonly utilized to simulate soil behavior. The preponderance of finite element programs only captures the structure's linear behavior (i.e., up to the yielding of the design). These programs fail to capture post-peak behavior (e.g., ultimate load-displacement responses, failure modes, and fracture patterns). The interaction between the pile shaft and the surrounding soil, on the other hand, is nonlinear. In addition to nonlinearity, the program should be able to capture the structure's post-peak reaction. As a result, choosing a program that can accommodate this behavior is essential. Unlike other programs **(Sharma et al., 2011)**, PLAXIS is a 3D nonlinear finite element software package that includes commonly used constitutive models to represent soil behavior, pile behavior, and the interface between pile and soil. PLAXIS can capture various pile structural conditions (e.g., static and seismic loads on the pile). Calculating the relationships between stress and strain in different soil models is one of the advantages of the PLAXIS-3D software, which allows loading and unloading behavior **(Polishchuk and Maksimov, 2017; Karkush et al., 2022)**. The most often used model for determining material plasticity is the Mohr-Coulomb model. It is a model that is linearly elastic and perfectly plastic. Hooke's law describes the linear elastic element. At the same time, the Mohr-Coulomb failure criterion represents the completely plastic part. When plastic deformations occur, irreversible strains or permanent deformations appear in the material yield function, which is introduced as a function that describes whether or not deformations occur. The material will stiffen or soften under plastic straining if the yield surface varies with plastic strain. As a result, a perfectly plastic model with a set yield surface is a constitutive model **(Gurtin and Anand, 2005; Taha et al., 2014)**.

To obtain accurate results with boundaries far from the distribution of stresses addressed from the applied loads, the boundary conditions are taken by sufficient measurements. The boundary conditions in both directions (X, Y) were 250 m, while the depth was 100 m, as shown in **Fig. 1**.

Interface elements are used to simulate the soil-structure interaction. The adjacent structural and soil elements may have to slide together if interface components are absent.

Between them, there is no relative movement (slipping or gapping). An interface can be created next to a plate, between two soil volumes or Geogrid. Interfaces in PLAXIS 3D are made up of 12-node interface elements after meshing (Spatial, 2021; Yao and Fujikubo, 2016). Node pairs make up interface elements. One node in a node pair is related to the structure, while the other is associated with the soil. The interaction between these two nodes defines the soil-structure interaction. It is made up of two perfectly elastic-plastic springs. The strength reduction factor ( $R_{inter}$ ) is used to point focal the strength of the interface. An elastic-plastic model describes the behavior of the interface (Tacioglu et al., 2006; Tradigo, 2016).

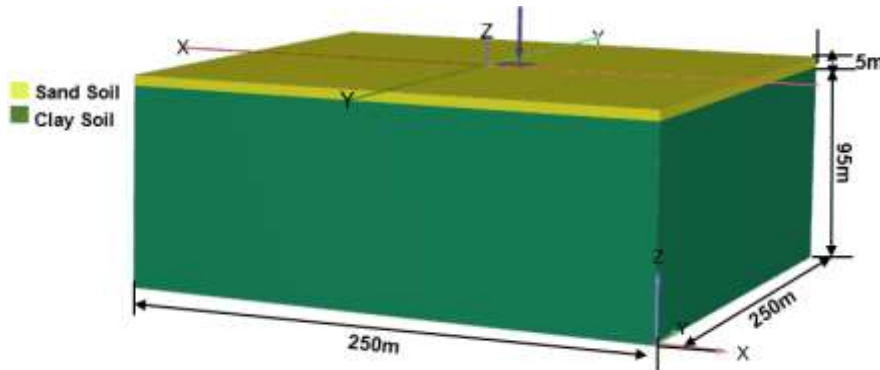


Figure 1. Modelling of boundary conditions.

The Mohr-Coulomb criteria is used to determine if an interface has failed. The following relationship can be used to compute the interface strength parameters (Datta et al., 2017),

$$C_i = R_{inter} \cdot C'_i \tag{1}$$

$$\tan \varphi'_i = R_{inter} \tan C'_i \tag{2}$$

where

$R_{inter}$  is the Interface factor.

$C_{inter}$  is the Cohesion of the interface (kN/m<sup>2</sup>).

$C'$  is the Cohesion of soil (kN/m<sup>2</sup>).

$\varphi_{inter}$  is the Friction angle of the interface (°).

$\varphi'_i$  is the Friction angle of the soil (°).

$R_{inter}$  is a program parameter that is either automatically determined by the software or manually selected by the user. When the first option is chosen, there will be no drop in interface strength compared to surrounding soil; strength and all other characteristics will remain unchanged, except the Poisson's ratio (Stoll, 1972; Yang, 2018).  $R_{inter}$  has a value equal to 1. This option is activated by default. The amount of  $R_{inter}$  is manually entered in the second option. In a real soil-structure interaction, the interface will be weaker and more flexible than soil, so  $R_{inter}$  has a value of less than 1. The appropriate  $R_{inter}$  value for interaction could be chosen based on the soil type. The strength reduction is more significant in cohesive soil than for cohesion-less soil, implying that the  $R_{inter}$  value for cohesion-less soil is more considerable. Whenever the interface strength reaches its limit value described by  $R_{inter}$ , it reduces to a residual strength characterized by  $R_{inter}$  residual strength (Ta and Small, 1996). When the third option is chosen, the  $R_{inter}$  residual is enabled, as shown in Fig. 2.

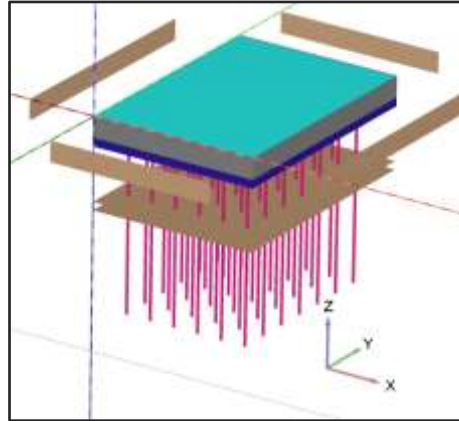


**Figure 2.** Modeling of interfaces.

when the geometry model is complete, it must be divided into finite elements. A mesh is a collection of finite elements. To obtain accurate results in the calculations that are carried out within the PLAXIS software, accurate meshes of soil and structure are used. However, they are not used with high accuracy, which leads to the use of significant times in the calculation. The program divided the model into 11867, an element and 19858, a node and type of mesh medium, as shown in **Fig. 3**.

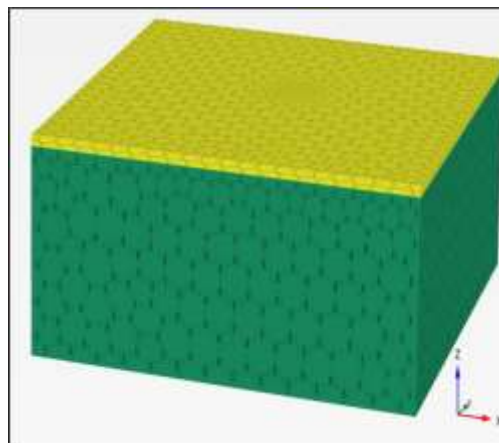


**Figure 3.** The adopted mesh.

### 3. Verification of the Numerical Model

To verify the proposed numerical model, a Messe-Torhaus Building Foundation, Frankfurt, 1983–1985, under static loading, was analyzed as an example of a piled-raft foundation (**Katzenbach et al., 2000**). The project is regarded as the first actual application of the heaped raft foundation for a high-rise structure in Germany to test the findings of the produced model (PLAXIS-3D model). As a result, during the building phase, a monitoring program was rigorously implemented to watch the behavior of the heaped raft. This structure consists of 30 stories, split into two rafts separated by 10 meters. The rafts are all 3 meters underneath and have a plan size of 17.5×24.5 m. The structural load is 200,000 kN, distributed evenly over the rafts at a stress of 466 kPa. The raft was 2.5 m thick and was attached to 42 drilled



piles with a diameter of 0.9 m and a length of 20 m, with the groundwater level being 3 m below ground level, as shown in **Fig. 4 (Katzenbach et al., 2000)**.

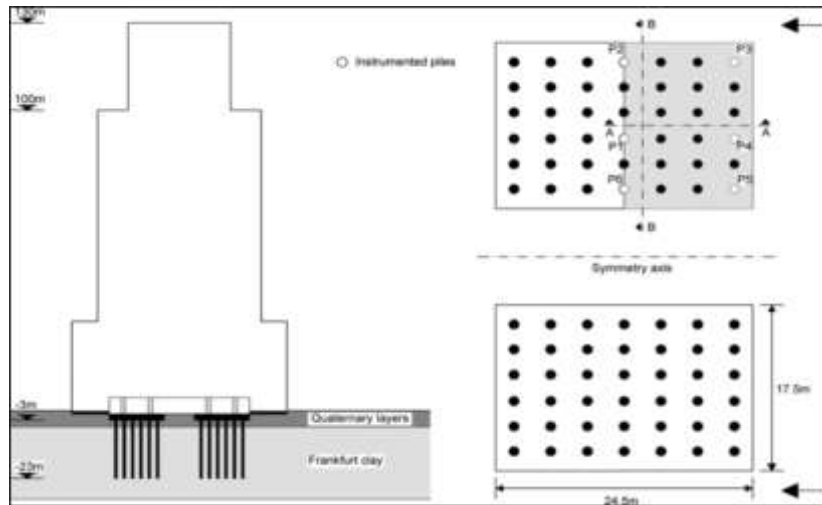


**Figure 4.** The piled raft system in the Messe-Torhaus building in Frankfurt (Katzenbach et al., 2000)].

The piles beneath each raft are evenly spaced in a 42-pile group with 3D to 3.5D spacing. **Fig. 5.** shows the subsurface profile, consisting of 5m of quaternary gravel and sand covering Frankfurt clay to a significant depth.

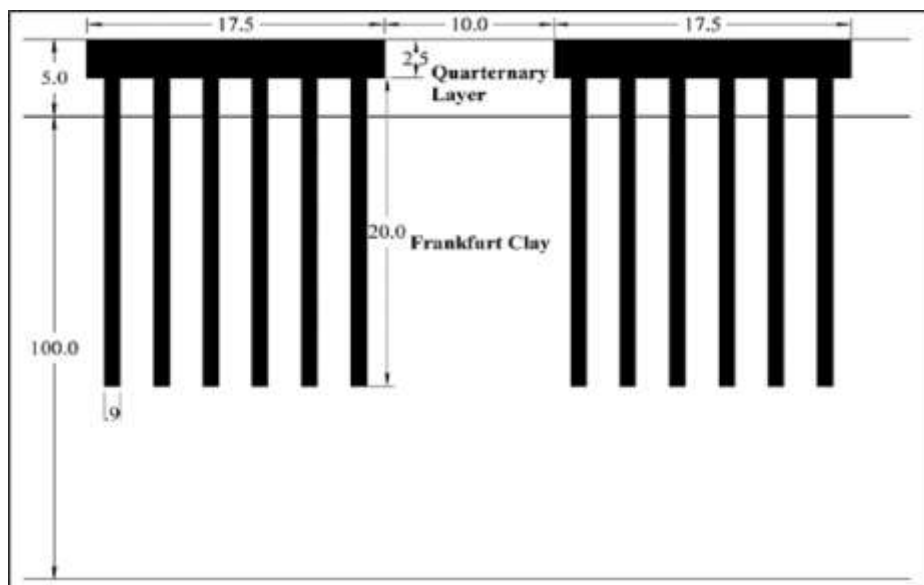


**Figure 5.** Soil layers for Messe-Torhaus structure foundation (Katzenbach et al., 2000).

The Mohr-Coulomb was dependent on the calculations of the soil material model, and the additional soil characteristics utilized in the PLAXIS-3D model are presented in two **Tables 1 and 2.** **Fig. 6** shows the piled-raft foundation used in PLAXIS-3D.

**Table 1.** Soil and piled raft important parameters for Messe-Torhaus building (Katzenbach et al., 2000).

Parameter	Quaternary gravel & sand	Frankfurt clay	Raft	Piles
Young's modulus, E (MPa)	75	50	34000	23500
Poisson ratio, $\nu$	0.25	0.35	0.2	0.2
Total unit weight (kN/m <sup>3</sup> )	18	19	25	25
Submerged unit weight (kN/m <sup>3</sup> )	-	9	-	-
Coefficient of lateral earth pressure at rest, $k_0$	0.72 ( $0 \leq z < 25$ ) 0.57 ( $z \geq 25$ )	0.46	-	-
The angle of internal friction, $\phi'$ , (°)	32.5	20	-	-
Cohesion, c (kPa)	0	20	-	-

(Reul and Randolph, 2002) presented an empirical equation to obtain the modulus of elasticity for the clay soils of the city of Frankfurt:

$$E = 45 + (\tanh(z - 3015) + 1) \times 0.7z \tag{3}$$

where E is the modulus of elasticity (MPa), and z is the depth below the surface (m).

**Table 2.** The cushion layer properties (Alhassani and Aljorany, 2020).

Property	Cushion layer	Property	Cushion layer
Modulus of elasticity, E (MPa)	60	Cohesion, c (kPa)	40
The angle of friction, $\phi$ (°)	19.4	Dry unit weight (kN/m <sup>3</sup> )	18.65

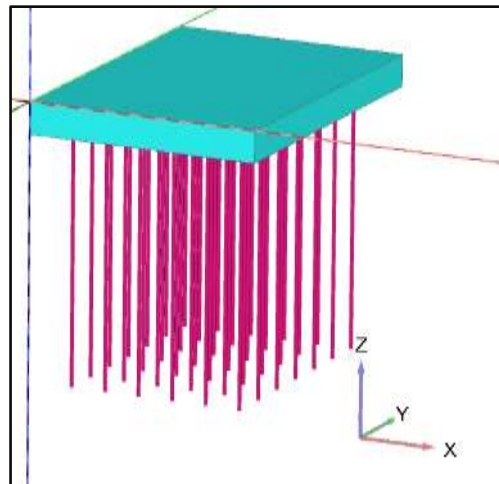


**Figure 6.** Messe-Torhaus building model used in PLAXIS software.

The maximum settlement caused by the building's weight is measured from the field was 154 mm, but the current study's settlement is 157 mm, as shown in Fig. 7. The difference between the current and field studies for the maximum settlement is 2%. In the foundation of the Messe-Torhaus building, the piles will be separated from the raft by a cushion layer made from the sand, as shown in Fig. 8. Also, the effect of reinforcing the cushion layer by

geogrid has been investigated using the finite element method in the PLAXIS-3D program. The properties cushion layer are given in **Table 2**. A raft was separated from the pile foundation by a cushion but for the same analysis of the foundation of the Messe-Torhaus building. The dimensions of the foundation were a 2.5 m thick rectangle raft having an area of 482.75 m<sup>2</sup> supported on 42 disconnected piles, the distance between the piles 3D to 3.5D, from pile diameter (0.9 m), and 20 m in length of the pile, the thickness of the cushion layer is 1m and the modulus of elasticity is 60 MPa (**Katzenbach et al., 2000**).

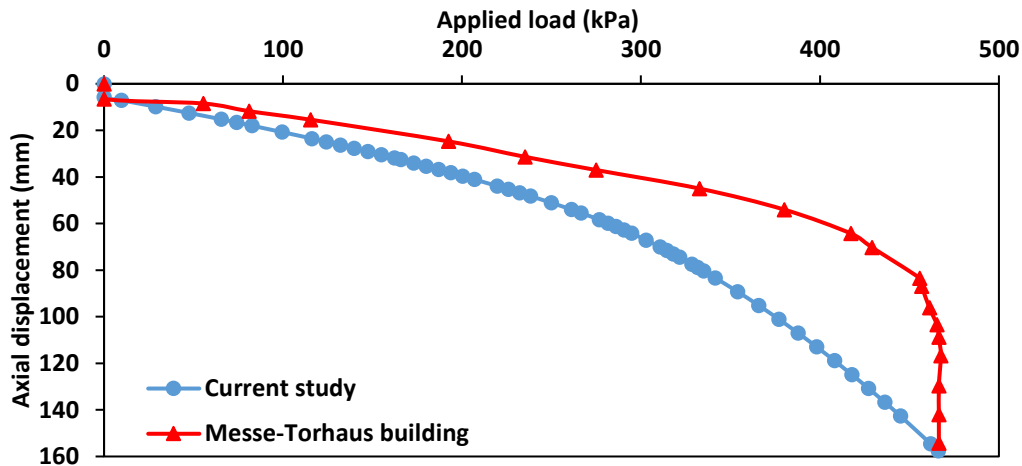


**Figure 7.** Verification of the settlement between the Messe-Torhaus building and current work.

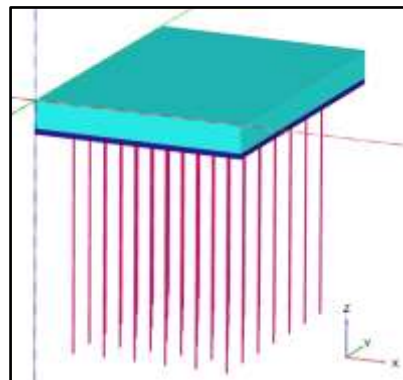


**Figure 8.** Disconnected piled raft model in PLAXIS 3D.

#### 4. SEISMIC LOADING

One of the most important and hazardous problems faced by geotechnical engineering is the presence of earthquakes that lead to damage or destruction of infrastructure, as they directly affect the stability of facilities and foundations (**Van der Sloot, 2019; Wei et al., 2008**). Therefore, it is necessary to design the foundations substantially that resist or limit the effect of earthquakes to preserve the safety of people from death. Recently, there has been an increasing interest in studying and understanding seismic phenomena and trying to predict the time of their occurrence. Despite many studies, there was no accurate information on determining the time of earthquakes because Iraq is located within the earthquake-prone areas. Many earthquakes hit Iraq over the years, where the eastern and northeastern regions

witnessed many earthquakes, while the southern and southwest regions are stable (**Tsuha et al., 2012**).

This study will depend on the earthquake that struck Iraq in November of 2017, in the (Halabja) region, killing many people and destroying many structures because of its strength as it was 7.3 on the Richter scale. Its impact reached Baghdad and acceleration ( $1 \text{ m/sec}^2$ ), as shown in **Fig. 9** (**Al-Taie and Albusoda, 2019**). In addition, the connected and disconnected piled raft foundations will be studied in this study under static and seismic loading.

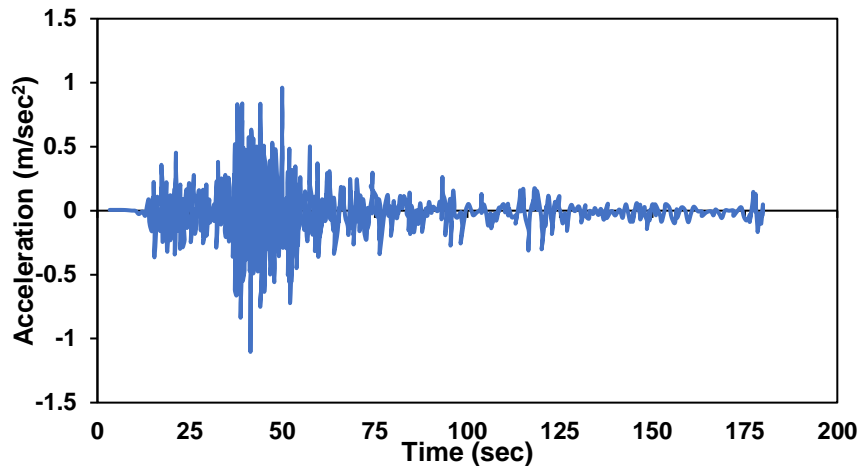


**Figure 9.** Acceleration–time history recorded in Baghdad for the Halabjah earthquake.

## 5. RESULTS AND DISCUSSION

The study's main objective is to verify the performance of the disconnected piled raft foundation same building under seismic loading and to calculate porous water pressure. And comparing these results with the foundation of the connected piled raft foundation under the same seismic load to know the effectiveness and behavior of the disconnected piled raft foundation.

### 5.1 Effect of Seismic Loading on Porewater Pressure

The influence of free water in the pores between the soil particles is another aspect to consider when applying loading to the foundation constructed on/in saturated soils. This free porewater is retained within the bounds of its local void during loading due to the impermeable character of clayey soils and the short period of dynamic loading. The soil particle-porewater system then handles load transmission. (**Terzaghi, 1943**) was the first who imagine the behaviour of a saturated clay subjected to loading.

To clarify the effect of the seismic load on the porewater pressure on the CPRF and DCPRF, the average readings at three nodes are taken in the soil at different depths (5, 11, 17, and 22.5 m) for CPRF and (5, 11, 17, and 23.5 m) for DCPRF. The groundwater level was 3 m below the soil surface, as shown in **Fig 10**.

**Figs. 11 to 18** show the variation of total porewater pressure during seismic loading on the CPRF and DCPRF at several depths. The total porewater pressure increases with increasing the length of the soil column.

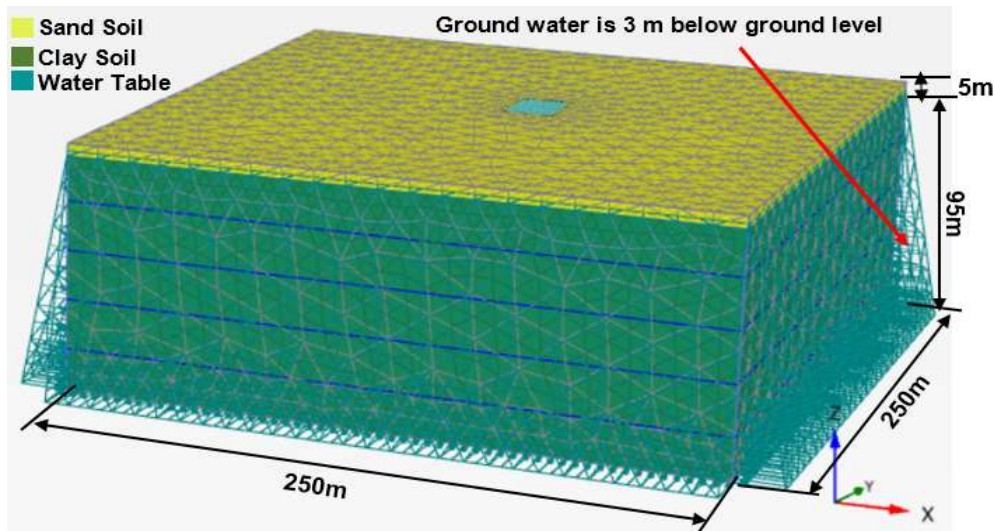


**Figure 10.** Distribution of porewater pressure of DCPRF under seismic loading.

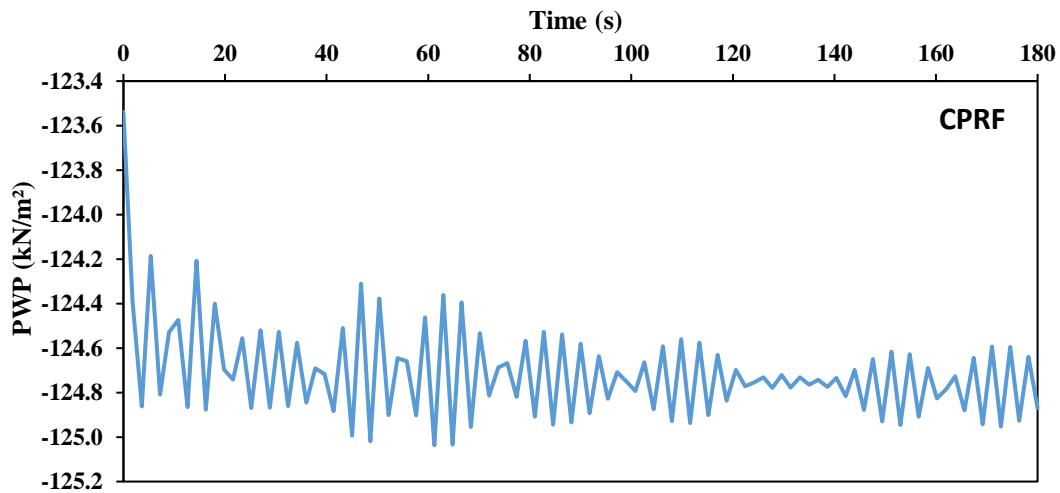


**Figure 11.** Total porewater pressure of CPRF under seismic load at depth 5 m.

It is observed in the case of a DCPRF, the porewater pressure in porous soil is much greater than in the case of a CPRF. The increase in the porewater pressure is due to the weight of the building and the weight of the additional cushion layer on the soil. The mechanism for transferring the load in the case of a DCPRF is carried out by raft, then to the cushion, and then to the soil and piles. The load transferred to the soil in the case of DCPRF is more than that transferred to the soil in the CPRF system.

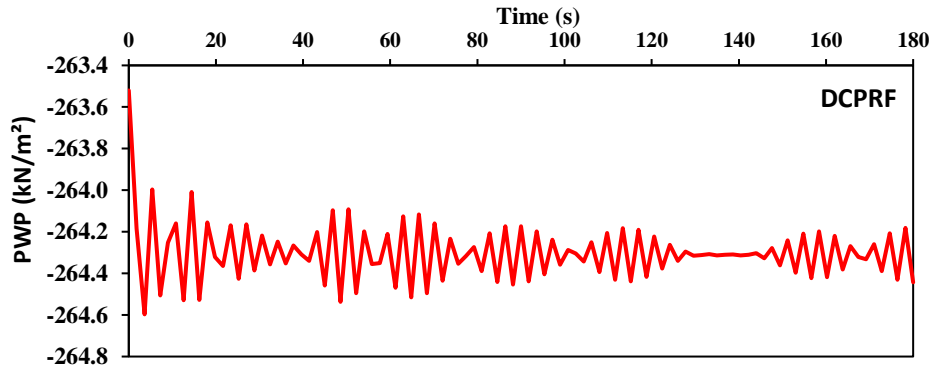


Figure 12. Total porewater pressure of DCPRF under seismic load at depth 5 m.

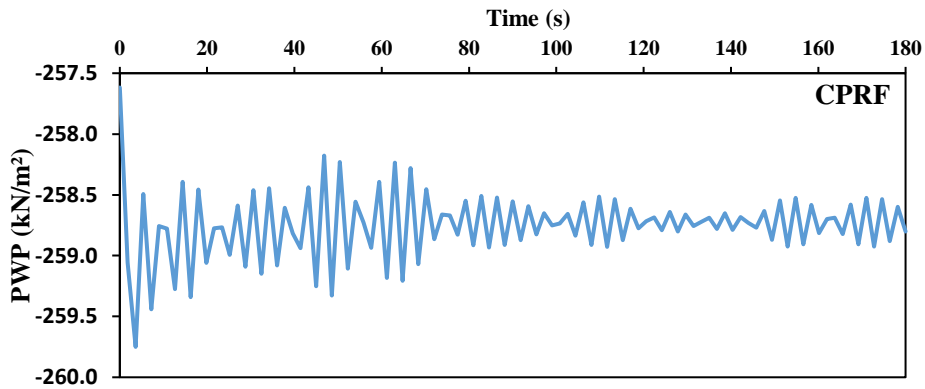


Figure 13. Total porewater pressure of CPRF under seismic load at depth 11 m.

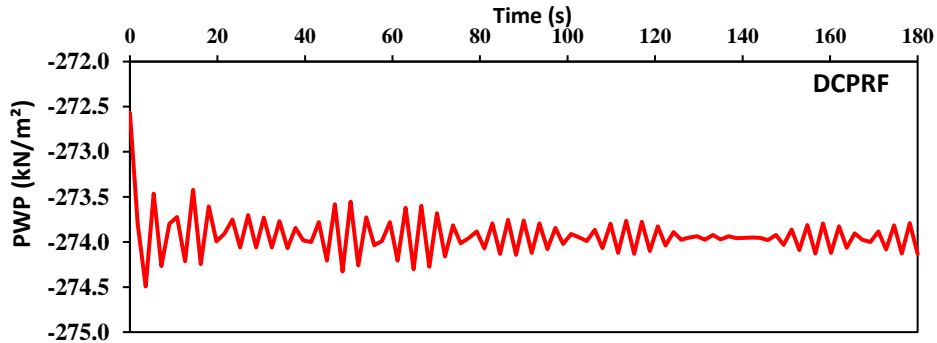


Figure 14. Total porewater pressure of DCPRF under seismic load at depth 11 m.

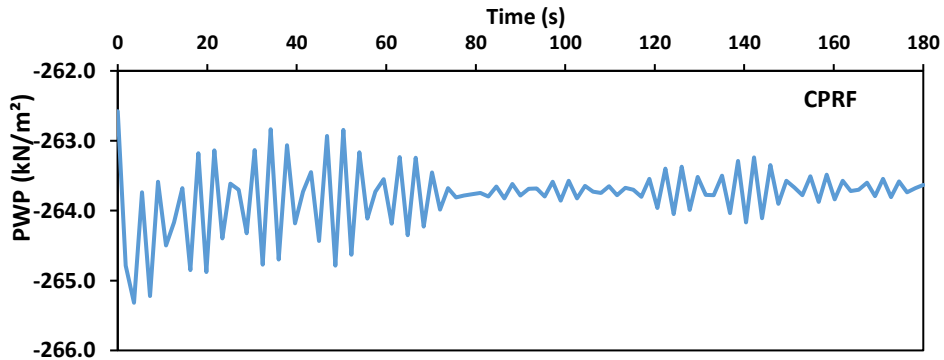


Figure 15. Total porewater pressure of CPRF under seismic load at depth 17 m.

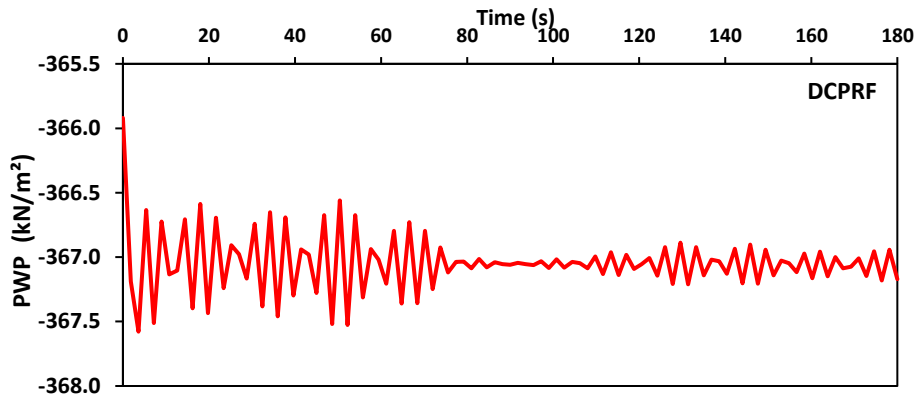


Figure 16. Total porewater pressure of DCPRF under seismic load at depth 17 m.

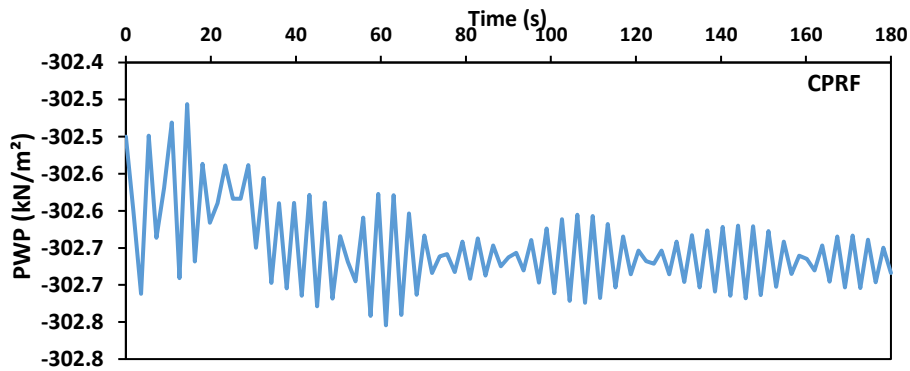


Figure 17. Total porewater pressure of CPRF under seismic load at depth 22.5 m.

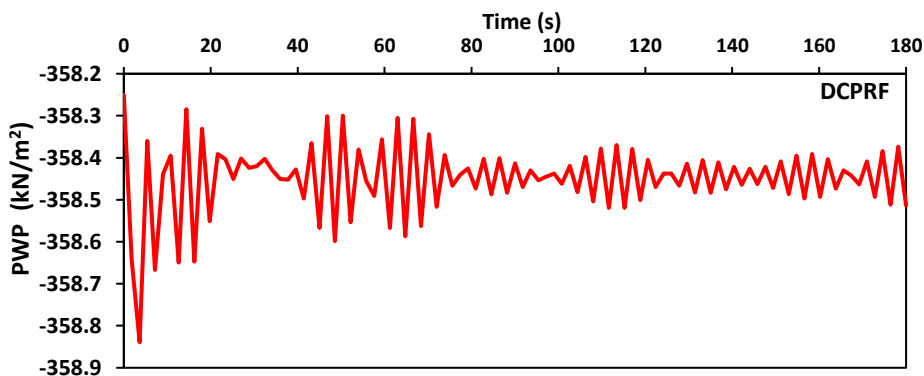


Figure 18. Total porewater pressure of DCPRF under seismic load at depth 23.5 m.

### 5.2 Effect of Seismic Loading on Excess Porewater Pressure

The excess porewater pressure is the pressure resulting from the sudden loading of soft soils, or what is called the undrained loading. Several depths were taken to study the effect of excess porewater pressure inside the soil mass. **Figs. 19 to 26** show the effect of the seismic loading on the extra porewater pressure on the CPRF and DCPRF at different depths (5, 11, 17, and 22.5 m) for CPRF and (5, 11, 17, and 23.5 m) for DCPRF. The amount of excess porewater pressure in the case of a DCPRF is much higher than in CPRF. This increase is due to an additional weight resulting from the weight of the cushion layer, where the load transfers from the weight of the building to the raft, then to the cushion layer and then to the



pile and soil below the cushion layer. Whereas in the case of a pile-connected foundation, the load transferred to the columns is more than it is in the soil under the raft.

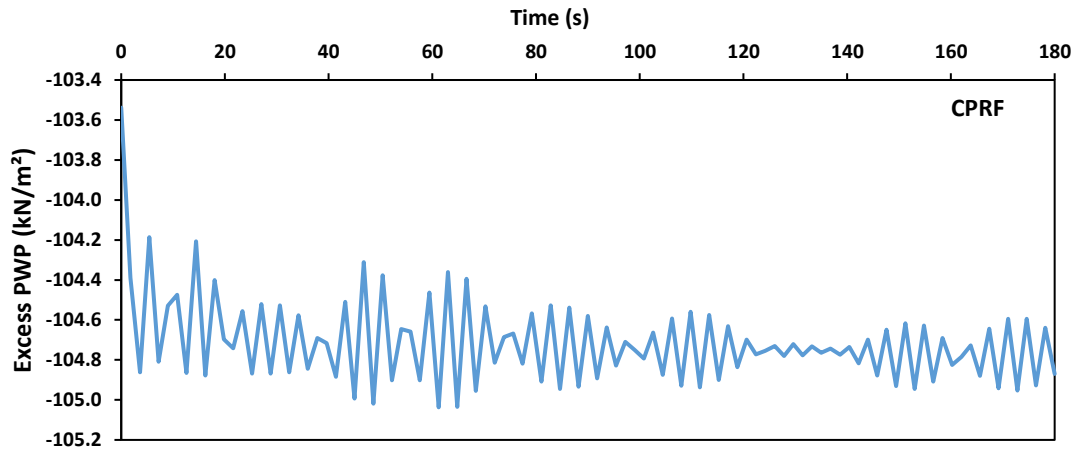


Figure 19. Excess porewater pressure of CPRF under seismic load at depth 5 m.

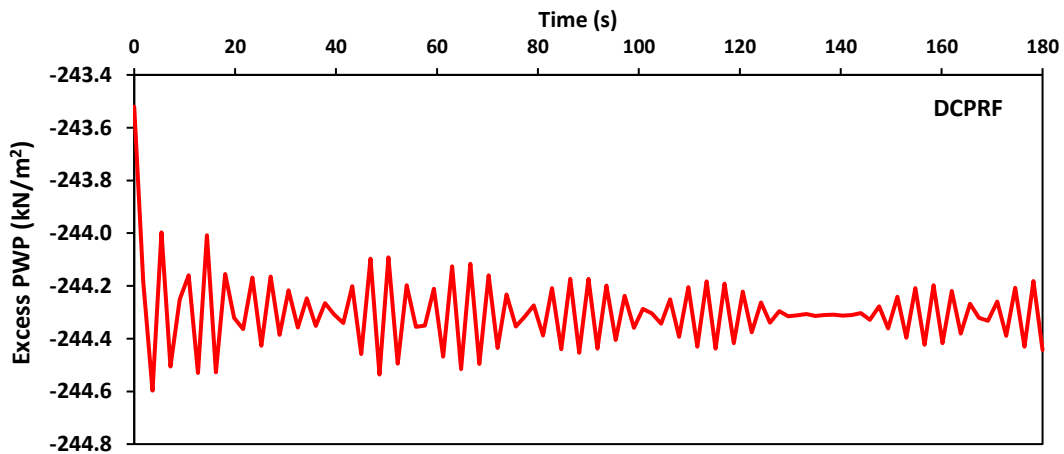


Figure 20. Excess porewater pressure of DCPRF under seismic load at depth 5 m.

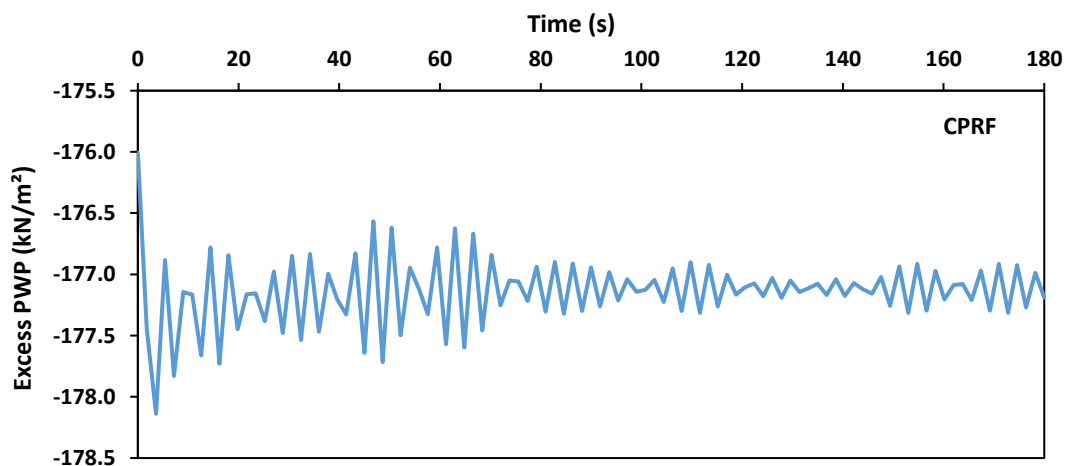


Figure 21. Excess porewater pressure of CPRF under seismic load at depth 11 m.

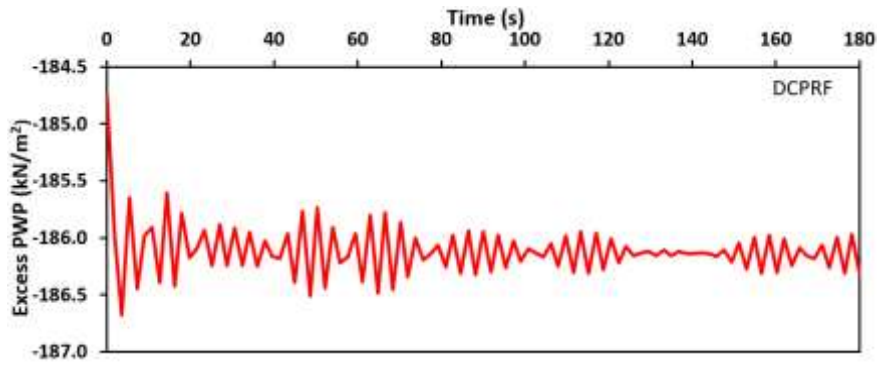


Figure 22. Excess porewater pressure of DCPRF under seismic load at depth 11 m.

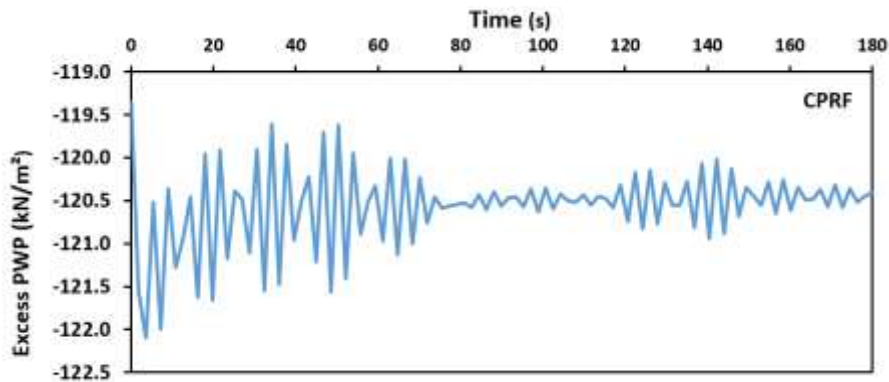


Figure 23. Excess porewater pressure of CPRF under seismic load at depth 17 m.

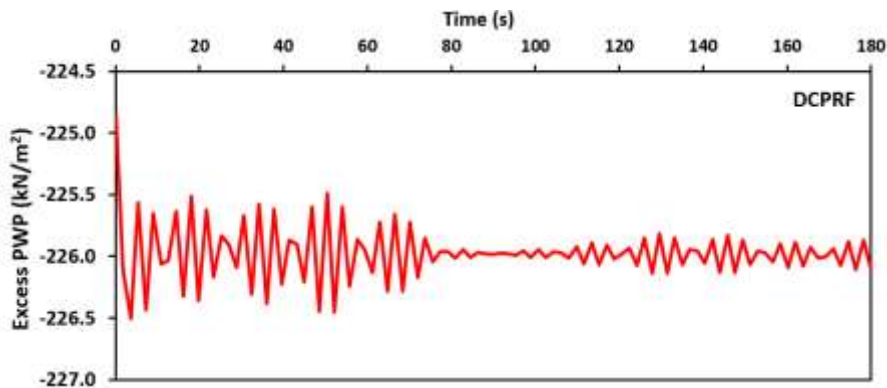


Figure 24. Excess porewater pressure of DCPRF under seismic load at depth 17 m.

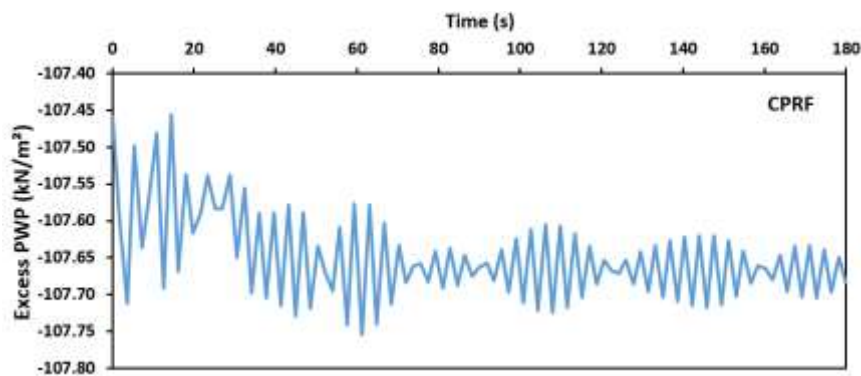
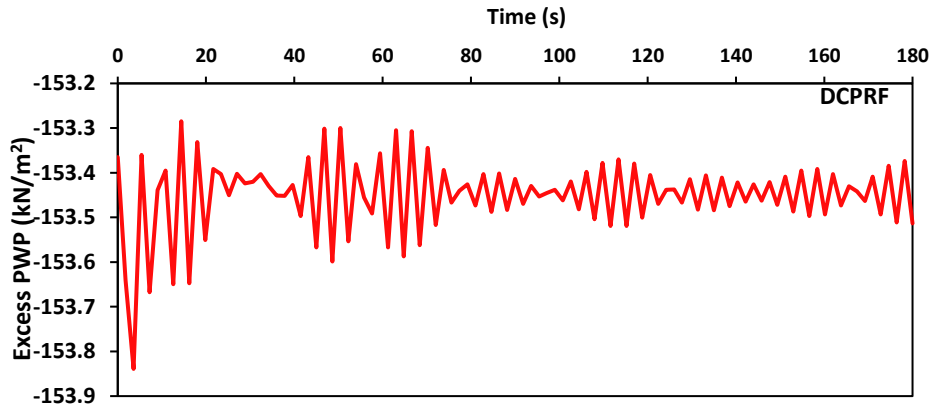


Figure 25. Excess porewater pressure of CPRF under seismic load at depth 22.5 m.



**Figure 26.** Excess porewater pressure of DCPRF under seismic load at depth 23.5 m.

## 6. CONCLUSIONS

The effect of seismic load on the pore water pressure in connected piled rafts and their foundations varies according to the measured depth are studied in this work. Per the previously discussed results the following conclusions can be reported:

1. The pore water pressure resulting from seismic loading of a DCPRF is 27% less than a CPRF at a node in the depth of 5m.
2. The pore water pressure resulting from seismic loading of a DCPRF is 67% less than a CPRF at a node in the depth of 11m.
3. The pore water pressure resulting from seismic loading of a DCPRF is 40% less than a CPRF at a node in the depth of 17m.
4. The pore water pressure increases with increasing depth.

## REFERENCES

- Alhassani, A.M., and Aljorany, A.N., 2020. Parametric study on disconnected piled raft foundation using numerical modelling. *Journal of Engineering*, 26(5), pp. 156-171. [Doi:10.31026/j.eng.2020.05.11](https://doi.org/10.31026/j.eng.2020.05.11).
- Al-Jeznawi, D., Jais, I.B.M., Albusoda, B.S., and Khalid, N., 2022. The slenderness ratio effect on the response of closed-end pipe piles in liquefied and non-liquefied soil layers under coupled static-seismic loading. *Journal of the Mechanical Behavior of Materials*, 31(1), pp. 83-89. [Doi:10.1515/jmbm-2022-0009](https://doi.org/10.1515/jmbm-2022-0009)
- Al-Kinani, A.M., and Ahmed, M.D., 2020. comparison of single and group bored piles settlement based on field test and theoretical methods. *Journal of Engineering*, 26(2), pp. 144-158. [Doi:10.31026/j.eng.2020.02.11](https://doi.org/10.31026/j.eng.2020.02.11).
- Al-Mosawe, M., Al-Shakarchi, Y., and Al-Saidi, A., 2007. Influence of defect in the concrete piles using non-destructive testing. *Journal of engineering*, 13(3), pp. 1804-1816.
- Al-Taie, A.J., and Albusoda, B.S., 2019. Earthquake hazard on Iraqi soil: Halabjah earthquake as a case study. *Geodesy and Geodynamics*, 10(3), pp. 196-204. [Doi:10.1016/j.geog.2019.03.004](https://doi.org/10.1016/j.geog.2019.03.004)
- Burland, J.B., Broms, B.B., and De Mello V.F.B., 1977. Behaviour of foundations and structures on soft ground. Proc. 9th ICSMFE, 1977, 2, pp. 495-546.



Datta, D, Varma, A.H, and Coleman, J., 2017. Investigation of interface nonlinearity on soil-structure interaction analyses. Transactions, SMiRT-24, 24th International Conference on Structural Mechanics in Reactor Technology Busan, South Korea.

Fioravante, V., 2011. Load transfer from a raft to a pile with an interposed layer. *Géotechnique*, 61(2), pp. 121-132. [Doi:10.1680/geot.7.00187](https://doi.org/10.1680/geot.7.00187)

Gurtin, M.E., and Anand, L., 2005. A theory of strain-gradient plasticity for isotropic, plastically irrotational materials. Part I: Small deformations. *Journal of the Mechanics and Physics of Solids*, 53(7), pp. 1624-49.

Karkush, M.O., and Ala, N.A., 2019. Numerical evaluation of foundation of digester tank of sewage treatment plant. *Civil Engineering Journal*, 5(5), pp. 996-1006. [Doi:10.28991/cej-2019-03091306](https://doi.org/10.28991/cej-2019-03091306)

Karkush, M.O., and Aljorany, A.N., 2020. Analytical and numerical analysis of piled-raft foundation of storage tank. Conference paper, *Construction in Geotechnical Engineering*, Lecture Notes in Civil Engineering, V. 84, pp. 373-384. Springer, Singapore. [Doi:10.1007/978-981-15-6090-3\\_26](https://doi.org/10.1007/978-981-15-6090-3_26)

Karkush, M.O., Ahmed MD, Sheikha AA, and Al-Rumaithi A., 2020. Thematic maps for the variation of bearing capacity of soil using SPTs and MATLAB. *Geosciences*, 10(9), P. 329. [Doi:10.3390/geosciences10090329](https://doi.org/10.3390/geosciences10090329)

Karkush, M.O., Ali, S.D., Saidik, N.M., and Al-Delfee, A.N., 2022 Numerical modeling of sheet pile quay wall performance subjected to earthquake. *Geotechnical Engineering and Sustainable Construction: Sustainable Geotechnical Engineering*, 19, P. 355. [Doi:10.1007/978-981-16-6277-5\\_28](https://doi.org/10.1007/978-981-16-6277-5_28)

Karkush, M.O., Sabaa, M.R., Salman, A.D., and Al-Rumaithi, A., 2022. Prediction of bearing capacity of driven piles for Basrah Governatore using SPT and MATLAB. *Journal of the Mechanical Behavior of Materials*, 31(1), pp. 39-51. [Doi:10.1515/jmbm-2022-0005](https://doi.org/10.1515/jmbm-2022-0005)

Katzenbach, R., Arslan, U., and Moormann, C., 2000. *Piled raft foundation projects in Germany*. InDesign applications of raft foundations, pp. 323-391. Thomas Telford Publishing.

Polishchuk, A.I., and Maksimov, F.A., 2017. Numerical analysis of helical pile–soil interaction under compressive loads. In IOP Conference Series: Materials Science and *Engineering*, 262(1), P. 012099. IOP Publishing.

Reul, O., and Randolph, M.F., 2002. Study of the influence of finite element mesh refinement on the calculated bearing behaviour of a piled raft. InProc. 8th International Symposium on Numerical Models in Geomechanics, pp. 259-264. [Doi:10.1201/9781439833797-c38](https://doi.org/10.1201/9781439833797-c38)

Shafique, M.A., Murtaza, G., Saadat, S., Uddin, M.K., and Ahmad, R., 2017. Improved cell viability and hydroxyapatite growth on nitrogen ion-implanted surfaces. *Radiation Effects and Defects in Solids*, 172(7-8), pp. 590-599. [Doi:10.1080/10420150.2017.1367296](https://doi.org/10.1080/10420150.2017.1367296)

Sharma, A., 2017. Modelling of Contact Interfaces using Non-homogeneous Discrete Elements to predict dynamical behaviour of Assembled Structures. PhD. Dissertation, Department of Mechanical Engineering, Technical University of Darmstadt.

Sharma, V.J., Vasanvala, S.A., and Solanki, C.H., 2011. Effect of cushion on composite piled raft foundation in layered soil under seismic forces. *International Journal of Scientific Engineering and Technology*, 1(6), pp. 314-322.

Spatial, 2021. An introduction to finite element modeling. [online] Blog.spatial.com. Available at: <https://blog.spatial.com/finite-element-modeling> [Accessed 14 May 2021]

Stoll, U.W., 1972. Torque shear test of cylindrical friction piles. *International Journal of Civil Engineering*, 42(4), pp. 63–65.



- Ta, L.D., and Small, J.C., 1996. Analysis of piled raft systems in layered soil. *International Journal for Numerical and Analytical Methods in Geomechanics*, 20(1), pp. 57-72. [Doi:10.1002/\(SICI\)1096-9853\(199601\)20:1<57::AID-NAG807>3.0.CO;2-0](https://doi.org/10.1002/(SICI)1096-9853(199601)20:1<57::AID-NAG807>3.0.CO;2-0)
- Taciroglu, E., Rha, C., and Wallace, J.W., 2006. A robust macroelement model for soil-pile interaction under cyclic loads. *Journal of geotechnical and geoenvironmental engineering*, 132(10), pp. 1304-1314. [Doi:10.1061/\(ASCE\)1090-0241\(2006\)132:10\(1304\)](https://doi.org/10.1061/(ASCE)1090-0241(2006)132:10(1304))
- Taha, A., El Naggat, M.H., and Turan, A., 2014. Experimental and numerical study on lateral behaviour of geosynthetic-reinforced pile foundation system. *Geosynthetics International*, 21(6), pp. 352-363. [Doi:10.1680/gein.14.00023](https://doi.org/10.1680/gein.14.00023)
- Terzaghi, K., 1943. Liner-plate tunnels on the Chicago (IL) subway. *Transactions of the American Society of Civil Engineers*, 108(1), pp. 970-1007. [Doi:10.1061/TACEAT.000566](https://doi.org/10.1061/TACEAT.000566)
- Tradigo, F., Pisanò, F., and di Prisco, C., 2016. On the use of embedded pile elements for the numerical analysis of disconnected piled rafts. *Computers and Geotechnics*, 72, pp. 89-99. [Doi:10.1016/j.compgeo.2015.11.005](https://doi.org/10.1016/j.compgeo.2015.11.005)
- Tsuha, C.D.H.C., Foray, P.Y., Jardine, R.J., Yang, Z.X., Silva, M., and Rimoy, S. 2012. Behaviour of displacement piles in sand under cyclic axial loading. *Soils and foundations*, 52(3), pp. 393-410. [Doi:10.1016/j.sandf.2012.05.002](https://doi.org/10.1016/j.sandf.2012.05.002)
- Van der Sloot, M., 2019. On different failure criteria for soils. <https://communities.bentley.com/products/geotech-analysis/w/plaxis-soilvision-wiki/45980/on-different-failure-criteria-for-soils>
- Wei, X., Wang, Q.Q., and Wang, J.J., 2008. Damage patterns and failure mechanisms of bridge pile foundation under earthquake. The 14th World Conference on earthquake engineering.
- Wong, I.H., Chang, M.F., and Cao, X.D., 2000. Raft foundations with disconnected settlement-reducing piles. Design applications of raft foundations, pp. 469-486. ICE Publishing Collection. [Doi:10.1680/daorf.27657.0017](https://doi.org/10.1680/daorf.27657.0017)
- Yang, K.H., 2018. *Stepping through finite element analysis*. Basic finite element method as applied to injury Biomechanics (pp. 281-308). Academic Press.
- Yao, T., and Fujikubo, M., 2016. *Buckling and ultimate strength of ship and ship-like floating structures*. Butterworth-Heinemann.
- Zhao, X.H., 1998. *Theory of design of piled raft & piled box foundations for tall buildings in Shanghai*. Tongji University Press.